Electronic structure of the Pu-based superconductor $PuCoGa_5$ and of related actinide-115 compounds

I. Opahle,[1] S. Elgazzar,[1,2] K. Koepernik,[1] and P. M. Oppeneer[1,3]
[1]*Leibniz-Institute of Solid State and Materials Research, P.O. Box 270016, D-01171 Dresden, Germany*
[2]*Department of Physics, Faculty of Science, Menoufia University, Shebin El-kom, Egypt*
[3]*Department of Physics, Uppsala University, Box 530, S-751 21 Uppsala, Sweden*
(Received 25 February 2004; revised manuscript received 8 June 2004; published 13 September 2004)

We report a theoretical investigation of the electronic structure of the plutonium-based medium-high-T_c superconductor $PuCoGa_5$, on the basis of *ab initio* local spin-density functional calculations. We furthermore report electronic structure calculations of the related actinide compounds $PuRhGa_5$, $PuIrGa_5$, $UCoGa_5$, $NpCoGa_5$, and $AmCoGa_5$. $PuRhGa_5$ is a superconductor as well, whereas the other materials do not become superconducting. The equilibrium lattice parameters within the tetragonal $HoCoGa_5$ crystal structure are well reproduced for $UCoGa_5$, $NpCoGa_5$, as well as for the three isoelectronic Pu-115 compounds when we assume delocalized $5f$ states. The possibility of a partial $5f$ localization occurring for the Pu-115 compounds is discussed. The electronic structures of the three Pu-115 compounds are computed to be rather similar: in each of the Pu-115 materials the density of states at the Fermi energy is dominated by the Pu $5f$ contribution. Our total-energy calculations predict antiferromagnetic order to be favorable for all three Pu-115 materials, which is, however, observed experimentally for $PuIrGa_5$ only. Within the Pu-115 series some small changes of the bands near the Fermi energy occur, which could be relevant for the superconductivity. A comparison of the *ab initio* calculated and the experimental properties clearly supports the picture of delocalized $5f$ electrons for $UCoGa_5$. The neptunium-based 115 compound is predicted to order antiferromagnetically, which is supported by experiment. Also, the calculated magnetic moment ($0.85\ \mu_B$) compares well with the measured moment ($0.84\ \mu_B$). These findings advocate that the Np $5f$'s are still to some extent delocalized in $NpCoGa_5$. In contrast, for the Am-115 analog the Am $5f$ electrons can be expected to be localized. We furthermore discuss the theoretical Fermi surfaces and present calculated de Haas-van Alphen quantities for a comparison with future experiments. For $UCoGa_5$ we obtain a semi-quantitative agreement with recently reported de Haas-van Alphen experiments. The possible origins of the superconductivity are discussed. Our investigation particularly reinforces the analogy to the heavy-fermion superconductors $CeCoIn_5$ and $CeIrIn_5$, however, with a stronger coupling strength due to a much stronger $5f$ hybridization.

DOI: 10.1103/PhysRevB.70.104504 PACS number(s): 74.70.−b, 71.28.+d

I. INTRODUCTION

An exciting new class of Pu-based superconductors was very recently discovered.[1,2] The original discovery—drawing worldwide attention—was that of superconductivity in $PuCoGa_5$ at an astonishingly high transition temperature of 18.5 K.[1] Before this discovery, no superconductivity in Pu-based materials was known to exist and most actinide superconductors exhibit T_c's of less than 2 K. Shortly after the initial discovery, superconductivity in the isoelectronic Pu compound $PuRhGa_5$ at a T_c of 8.5 K was reported.[2] Under pressure the T_c of $PuRhGa_5$ increases to 16 K while that of $PuCoGa_5$ raises to 23 K.[3] The first experimental results for the isoelectronic $PuIrGa_5$ indicate the absence of superconductivity (down to 2 K), but magnetic ordering is inferred from the susceptibility below 17 K.[4] After the discovery of superconductivity in $PuCoGa_5$, attention has also focused on other transuranium compounds, which crystallize in the same tetragonal $HoCoGa_5$ structure. $NpCoGa_5$ orders antiferromagnetically below $T_N=47$ K and does not become superconducting.[5] Preliminary results for $AmCoGa_5$ indicate this material to be a temperature-independent paramagnet with no sign of superconductivity down to 2 K.[6] Also, a number of related uranium-115 materials have been prepared and studied before the superconductivity in $PuCoGa_5$ was discovered.[7–14] The isostructural analogs $UCoGa_5$ and $URhGa_5$ were reported to be nonsuperconducting, temperature-independent paramagnets,[7,9,11] while $UNiGa_5$ and $UPtGa_5$ order antiferromagnetically and display a weakly-temperature dependent magnetic susceptibility above the respective Néel points.[13,15] Especially from the findings for the Pu-115 materials, it seems that the newly-discovered superconductivity appears in a class of materials that are on the verge of magnetic ordering. This observation bears on the possible nature of the pairing mechanism (see, e.g., Ref. 16). The unprecedented, high T_c as well as the proximity to magnetic ordering raises the question if possibly an unconventional pairing could be operative.

Three years prior to the report on Pu-based superconductivity a related group of heavy-fermion superconductors, crystallizing in the same $HoCoGa_5$ structure, was discovered. To this group belong the Ce compounds $CeCoIn_5$, $CeRhIn_5$, and $CeIrIn_5$.[17–19] $CeCoIn_5$ and $CeIrIn_5$ were found to be superconductors at ambient pressure,[18,19] with $T_c=2.3$ and 0.4 K, respectively, whereas $CeRhIn_5$ becomes a superconductor (with $T_c=2.1$ K) under pressure.[17] At ambient pressure $CeRhIn_5$ orders antiferromagnetically with an incommensurate spin spiral below the Néel temperature T_N

=3.9 K.[20] On account of the unusual interplay of heavy-fermion behavior, magnetic ordering, and superconductivity an unconventional pairing mechanism has been envisaged.[18,19] Indeed, very recently several experimental evidences for unconventional, spin-singlet *d*-wave superconductivity in $CeRhIn_5$ and $CeCoIn_5$ were presented.[21–24] These findings for the Ce-115 superconductors bear certainly relevance for the physics of the Pu-115 superconductors, the investigation of which is only just commencing.

Undoubtedly, a challenging task for the future is unraveling the nature of the unprecedented superconductivity in $PuCoGa_5$. To this end more experimental information is pressingly needed, which, however, is burdensome to acquire because of the radioactivity of Pu and its handling restrictions. Another approach is to investigate the electronic structure by first-principles calculations. The underlying electronic structure bears relevance to the superconductivity, since it reveals, e.g., what kind of electrons form the Cooper pairs and what the topology of the Fermi surface is. These aspects were studied in two recent short-note publications.[25,26] The electronic structure calculations predicted the energy bands at the Fermi energy (E_F) to consist dominantly of delocalized Pu $5f$ states and the Fermi surface of $PuCoGa_5$ was predicted to have an anisotropic, quasi two-dimensional shape.[25] In contrast, $UCoGa_5$ was calculated to exhibit rather a three-dimensional Fermi surface.[26] These are important aspects, however, in order to obtain a more complete understanding of the electronic structure of the Pu-115 and related actinide-115 compounds, further electronic structure investigations are certainly desirable.

We report here extensive *ab initio* calculations of electronic properties of $PuXGa_5$ (X=Co, Rh, and Ir), $NpCoGa_5$, $UCoGa_5$, and $AmCoGa_5$. We performed state-of-the-art full-potential, relativistic total-energy calculations to determine the theoretical equilibrium lattice parameters, which we optimized considering different, possible magnetic phases. Furthermore, we investigate the energy-band structure, the character of the states near the Fermi energy, the density of states, and the Fermi surfaces. Also, we present calculated de Haas-van Alphen (dHvA) quantities for the Pu-115 compounds and for $UCoGa_5$.

All our calculations utilize the local spin-density approximation (LSDA) to density-functional theory. Because of its derivation from the homogeneous electron gas, the LSDA is appropriate for delocalized electrons. It provides a good description of the bonding in the early actinide elements,[27] but precisely for Pu difficulties are known to occur. Right at Pu, a transition occurs in the actinide series from delocalized $5f$ behavior in the lighter actinides (e.g., U and Np) to localized $5f$ behavior in the heavier actinides (Am and beyond) (see, e.g., Ref. 28). Thus, the behavior of the Pu $5f$ electrons is often intermediate to localized and delocalized, a situation which cannot easily be captured by theoretical approaches. The prime example of such challenge is elemental Pu. The α-phase of elemental Pu is rather well explained by LSDA calculations (see, e.g., Ref. 29), but for the δ-phase of Pu the appropriate approach is still a matter of debate.[30–35] Hybridization effects may modify the localization behavior of the $5f$'s in the case of Pu compounds. It has been found, for example, that the Pu $5f$'s are rather localized in PuSb,[36] whereas for PuSe and PuTe the $5f$'s appear to be relatively delocalized.[37–39] Very recently, it was shown that the localization degree of the Pu $5f$'s is important, too, for $PuCoGa_5$. Photoemission experiments[40] revealed a delocalized $5f$ response near the Fermi energy, as well as a second response at 1.1 eV binding energy, which was attributed to localized $5f$ states. Here we adopt the delocalized LSDA approach for the lighter actinide-115 and the Pu-115 compounds, while we treat the Am $5f$ electrons of $AmCoGa_5$ as core electrons. The validity of the LSDA description will be discussed. Where possible, we compare calculated electronic structure properties to the available experimental data. To shed more light on the nature of the Pu $5f$ electrons in the Pu-115 compounds further comparisons between calculated and measured quantities will be required. As one step in this direction we provide calculated de Haas-van Alphen frequencies and masses.

In the following we first outline our computational approach. In Sec. III we present our obtained results, first for the $PuXGa_5$ (X=Co, Rh, and Ir) compounds, and subsequently, for $UCoGa_5$, $NpCoGa_5$, and $AmCoGa_5$.

II. COMPUTATION ASPECTS

Our calculations were performed using the relativistic version[41,42] of the full-potential local orbital (FPLO) minimum-basis band-structure method.[43] In this scheme the 4-component Kohn-Sham-Dirac equation, which implicitly contains spin-orbit coupling up to all orders, is solved self-consistently. As a basis set Bloch sums of atom-like local orbitals are used. The local orbitals are chosen as solutions of a single particle Dirac equation in the spherically averaged crystal potential and an additional confining potential, which is applied to valence states only. The confining potential contains an orbital dependent variational parameter which is used to adjust the local basis states such that the total energy is minimized. It has the purpose both to compress the local valence orbitals and to shift their energy, so that it comes close to the band centers, thus providing an optimized basis for the construction of extended states. For the present calculations, we used the following basis sets: for U, Np, and Pu the $5f;6s6p6d;7s7p$ states were chosen as valence states, while for Ga we used $3d;4s4p4d$. For Co we used the $3d;4s4p$ states and equivalent sets with higher quantum numbers for Rh and Ir. For the actinides the high-lying $6s$ and $6p$ semicore states are included in the basis. These semicore states might hybridize with the $6d$ and $5f$ valence states. The site-centered potentials and densities were expanded in spherical harmonic contributions up to $l_{max}=12$. The number of *k*-points in the irreducible part of the Brillouin zone was 196, but calculations were made also with 405 and up to 2176 *k*-points to resolve the density of states at E_F. The Perdew-Wang[44] parametrization of the exchange-correlation potential in the local spin-density approximation (LSDA) was used.

The actinide-115 compounds all crystallize in the $HoCoGa_5$ structure ($P4/mmm$ space group), shown in Fig. 1. The unit cell of this tetragonal structure can be viewed as derived from the cubic $HoGa_3$ unit cell, which has been elongated along the *c* axis by an extra layer of $CoGa_2$ being built

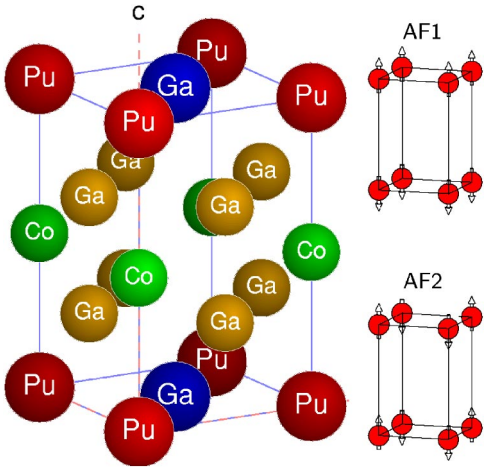

FIG. 1. (Color online) Crystal structure of $PuCoGa_5$ (left) and schematic view of the two considered antiferromagnetic arrangements (see the text) showing the magnetic moments on the actinide atoms.

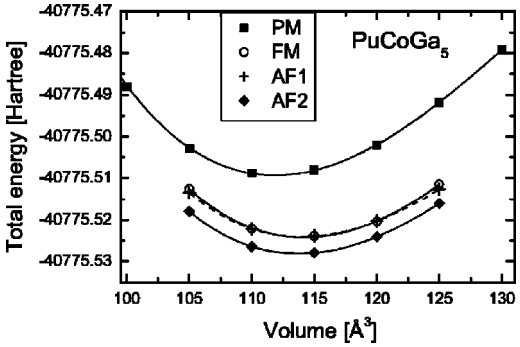

FIG. 2. Calculated total energy as a function of volume for $PuCoGa_5$ in the paramagnetic (PM), ferromagnetic (FM), and in two antiferromagnetic phases (AF1 and AF2, respectively; see text).

in.[19] The unit cell has one specific, internal Ga z coordinate. The three theoretical equilibrium lattice parameters a, c/a, and the specific Ga z coordinate were determined by total-energy minimization. This procedure was carried out adopting several possible magnetic phases for the Pu-115 compounds. We have considered the paramagnetic (PM) phase, the ferromagnetic phase (FM), as well as two antiferromagnetic (AF) phases. Within the $HoCoGa_5$ structure, which is quasi-two-dimensional containing actinide-Ga planes having a large interplane separation, two of the most essential AF configurations are as follows. All the actinide atoms within one layer can be ferromagnetically ordered along the c axis, but antiferromagnetically coupled to the adjacent layer. Thus, the antiferromagnetic $\boldsymbol{Q}$-vector is (0 0 1/2). This type of antiferromagnet is denoted here as AF1 (see Fig. 1). This ordering-type has, for example, been observed for $UPtGa_5$.[15] The second AF arrangement is that where the nearest-neighboring actinide atoms in one layer are all antiferromagnetically coupled to one another, whereas the interlayer coupling is ferromagnetic. The $\boldsymbol{Q}$-vector is thus (1/2 1/2 0). This type of antiferromagnet, which we shall denote as AF2, is closely related to the Néel ordering found,[15] for example, in $UNiGa_5$ [which has $\boldsymbol{Q}=(1/2\ 1/2\ 1/2)$]. In the latter AF structure also the actinide layers are coupled antiferromagnetically along the c axis. Previously we calculated the magnetic coupling of adjacent Pu planes to be very weak,[25] therefore we do not expect a significant dependence on the magnetic modulation along the c axis.

III. RESULTS

A. $PuCoGa_5$

The first electronic structure results were already presented for $PuCoGa_5$ (Refs. 25 and 26), which we shall not repeat here. The theoretical equilibrium lattice parameters were not yet determined for the AF2 phase. In Fig. 2 we show the calculated total energy *versus* volume for the four considered magnetic phases. From Fig. 2 we observe that AF2 has a lower total energy than AF1. Thus, antiferromagnetic coupling of the nearest-neighboring actinide moments within one layer is more favorable than ferromagnetic coupling. The Pu-Pu interplane magnetic coupling is very weak, as follows from the near-energy degeneracy of the FM and AF1 phases. This finding is in accordance with the quasi-two-dimensional crystal structure. The computed equilibrium lattice parameters of the AF2 phase are practically the same as those computed for the FM and AF1 phases. The computed values $a=4.15$ Å, $c/a=1.602$, and $z(\mathrm{Ga})=0.304$ compare well with the experimental lattice parameters,[1] $a=4.232$ Å, $c/a=1.603$, and $z(\mathrm{Ga})=0.312$, respectively.[45] Adopting the LSDA delocalized $5f$ description leads thus to a reasonably good explanation of the lattice parameters of $PuCoGa_5$. The error in the theoretical lattice constant (being 1.9% smaller than the experimental one) is quite typical for LSDA-based calculations. A lattice constant approaching closer the experiment can be expected from generalized gradient approximation (GGA) calculations, which usually improve on the overbinding of the LSDA.

Susceptibility measurements[1] provided so far no evidence for AF ordering in $PuCoGa_5$. The temperature dependence of the resistivity, however, shows an S-like shape indicative of scattering due to spin fluctuations. The susceptibility obeys a modified Curie-Weiss behavior at elevated temperatures with an effective moment of 0.68 μ_B. The latter value indicates local moment behavior close to that expected for a Pu^{3+} ion ($\mu_{eff}=0.84\ \mu_B$).[46] The Pu^{3+} ion (i.e., $5f^5$ configuration) has one hole in the $5f_{5/2}$ subband and is therefore expected to be magnetic. There are several possibilities why no magnetic ordering is observed down to about 20 K. It could be that above T_c the AF order is dynamically washed out by spin fluctuations or by Kondo-type screening of the Pu moment. The experimental[1] specific-heat coefficient $\gamma \approx 60-77$ mJ/molK^2 is similar or somewhat higher than that of δ-Pu and four times enhanced compared to that of α-Pu (Ref. 47). Thus, many-particle correlations are definitely present. Below about 20 K it could be that AF order and superconductivity are competing orders. The occurrence of AF order

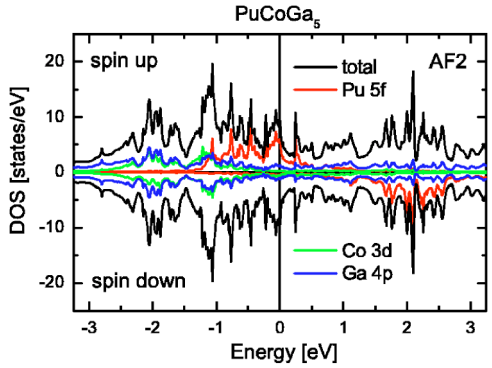

FIG. 3. (Color online) Calculated total and partial density of states (DOS) of $PuCoGa_5$ in the AF2 phase, for the experimental lattice parameters. Note that the spin-projected partial DOS of only one AF type of atom is plotted, as the DOS of the second AF atom-type is identical, but with spin up and spin down DOS interchanged.

at $T<T_c$ could possibly be suppressed by the electron pair formation.

In Fig. 3 we show the calculated partial DOS of $PuCoGa_5$ in the AF2 phase (for the experimental lattice constants). The partial DOS of the AF2 phase is rather similar to that of the AF1 phase.[25] The dominant contribution to the total DOS in the vicinity of E_F stems from the Pu $5f$ states. The Co $3d$ states are rather localized and occur moderately deep below E_F, at a binding energy of $1-2.5$ eV. The Ga $4p$ states are very dispersive, extending from -5 eV to above 5 eV. Near the Fermi level the main hybridization occurring is that of Pu $5f$ and Ga $4p$ states.

The energy bands of $PuCoGa_5$ depend moderately on the lattice parameters. Previously we computed the energy bands and Fermi surface of paramagnetic $PuCoGa_5$ for the theoretical equilibrium lattice parameters.[25] In Fig. 4 we show the band structure of paramagnetic $PuCoGa_5$ in the vicinity of E_F for the experimental lattice constants. For a comparison to be given below, the energy bands of $PuRhGa_5$ and $PuIrGa_5$ are also shown in Fig. 4. The bands near the Fermi level consist dominantly of Pu $5f$ character.[25] The calculations reveal that there is one band crossing along the $\Gamma-X$ direction which is sensitive to changes in the lattice parameters and numerical details of the calculation, as well as a band dispersion about the M point. Changes in the latter band effectually give rise to a modification of the topology of the corresponding Fermi surface sheet for $PuCoGa_5$. Modifications of the former band lead to differences within the corresponding Fermi surface sheets of the three Pu-115 materials.

The calculated Fermi surface of paramagnetic $PuCoGa_5$ is shown in Fig. 5, for the experimental lattice constants. The colors of the Fermi surfaces indicate the relative sizes of the Fermi velocities (i.e., $\partial E/\partial k$) on the sheets. A high Fermi velocity is expressed by the red color, a small Fermi velocity by the dark blue color. There are four bands crossing E_F, giving rise to five Fermi surface sheets: A spherically-shaped hole pocket centered at the Γ point, a disjunct Fermi surface

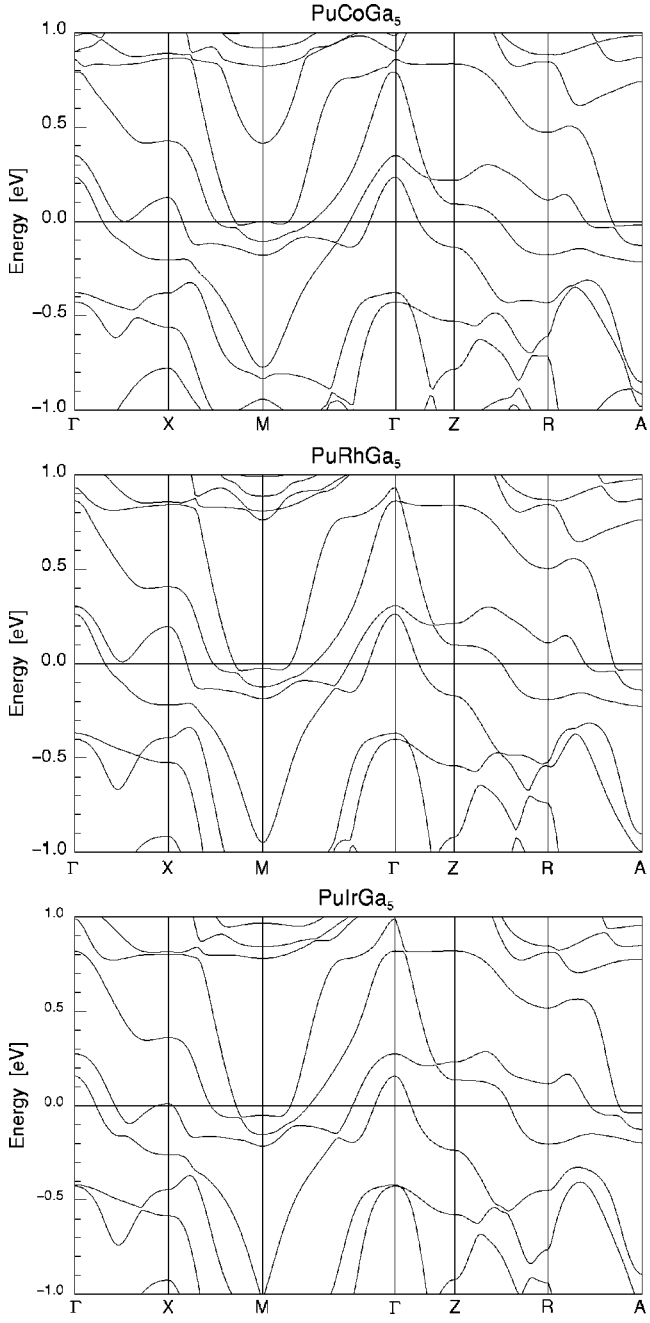

FIG. 4. Calculated energy bands of paramagnetic $PuCoGa_5$, $PuRhGa_5$, and $PuIrGa_5$, respectively, for the experimental lattice parameters.

portion consisting of an X centered, hole ellipsoid and one somewhat rectangular hole tube along the z axis. The fourth sheet is a rectangular electron tube along the $A-M-A$ edge of the Brillouin zone. The fifth sheet is also an electron tube-like structure along the $A-M-A$ edge. Only the two small hole pockets have a three-dimensional shape, otherwise the Fermi surface is distinctly two-dimensional. The main modification of the Fermi surface with the lattice parameters occurs for the fifth Fermi sheet, which, for the theoretical lattice constants was partially open in the $z=0$ plane.[25] This

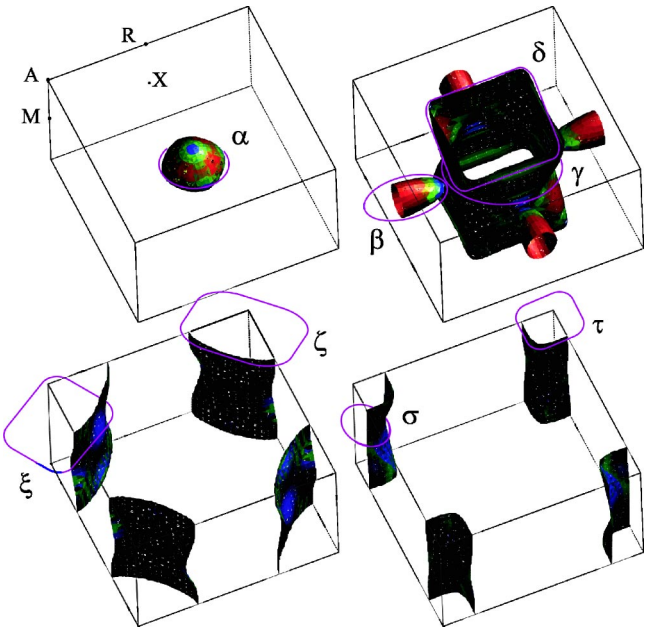

FIG. 5. (Color online) Calculated Fermi surface of paramagnetic $PuCoGa_5$ with extremal orbits for a field along the *c* axis indicated by Greek letters. Apart from the two small hole pockets at the Γ point and at the *X* points, the Fermi surface sheets are pronouncedly two-dimensional. Colors depict the size of the Fermi velocity: blue corresponds to a small velocity, red to a large Fermi velocity.

sheet becomes a closed, tube-like surface for the experimental lattice parameters. Thus, this Fermi surface sheet becomes more two-dimensional for the larger lattice constants. The *ab initio* calculated Fermi surface is rather simple, therefore it should not be difficult to identify the various Fermi surface sheets experimentally, for example in de Haas-van Alphen measurements. The two-dimensionality of the tubes, e.g., would immediately show up in the extremal cross sections once the field is rotated away from the *c* axis. Recently, dHvA experiments provided vital information concerning the Fermi surface topology of the Ce-115 heavy-fermion superconductors[48–50] and of some U-115 compounds.[11,51] For the Pu-115 materials investigations of the dHvA quantum oscillations have not been carried out as yet, but experiments are scheduled. In Table I we provide, for future comparison, calculated[52] values for the dHvA frequencies *F* (i.e., extremal cross sections) and effective masses *m*. The extremal orbits for a magnetic field along the *c* axis are indicated in Fig. 5 and labeled with Greek letters. The two closed hole Fermi surface sheets (α and β) depend significantly on the lattice parameters, which, understandably, is related to their relatively small sizes.

B. $PuRhGa_5$

$PuRhGa_5$ was the second Pu-based material discovered[2] to become superconducting at 8.5 K. Under pressure a T_c of maximally 16 K has been obtained.[3] The electronic structure of $PuRhGa_5$ was not yet investigated. In Fig. 6 we show the results of the total energy *versus* volume calculations for the

TABLE I. Calculated de Haas-van Alphen frequencies *F* and orbital masses *m* of paramagnetic $PuCoGa_5$ for a magnetic field parallel to the *c* axis. The greek symbols labeling the extremal orbits are shown in Fig. 5. Computed dHvA quantities are given for the theoretical as well as experimental lattice parameters. The dHvA frequencies of the extremal orbits are given in kT and their masses in units of the electron mass.

		Theo. latt. param.		Exp. latt.param.	
Symbol	Center (band)	*F* (kT)	*m* (m_e)	*F* (kT)	*m* (m_e)
α	Γ(87)	0.741	−0.778	1.476	−1.098
β	*X*(89)	0.929	−1.224	1.371	−2.494
γ	Γ(89)	4.984	−3.199	4.468	−5.720
δ	*Z*(89)	6.655	−3.450	5.361	−3.804
ξ	*M*(91)	4.930	4.658	4.752	4.414
ζ	*A*(91)	6.343	3.921	5.468	3.724
σ	*M*(93)	—	—	1.458	1.973
τ	*A*(93)	2.028	1.395	2.248	1.274

PM, FM, and AF2 phases. Since we found the results for the AF1 and FM phases always to be very close to one another, we do not show results for AF1 anymore. Also for $PuRhGa_5$ we find the AF2 phase to have the lowest total energy. The calculated equilibrium lattice parameters are: $a=4.239$ Å, $c/a=1.590$, and $z(\mathrm{Ga})=0.298$, which are to be compared to the experimental data $a=4.3012$ Å, $c/a=1.594$, and $z(\mathrm{Ga})=0.3064$, respectively. The theoretical lattice parameter *a* is only 1.5% smaller than the experimental one. Investigations of $PuRhGa_5$ are only just beginning to be undertaken, but so far AF ordering has not been observed.[4] The temperature-dependence of the measured resistivity shows—similar to $PuCoGa_5$—an upturn at about 100 K, typical of spin fluctuations.[2] The susceptibility obeys a modified Curie-Weiss law with an effective moment 0.60 μ_B, which is somewhat reduced with respect to the Pu^{3+} value.[2] Thus, the physical properties of $PuRhGa_5$ are comparable to those of $PuCoGa_5$.

The calculated DOS of $PuRhGa_5$ is shown in Fig. 7 for the experimental lattice parameters. The DOS of the PM phase is rather similar to that of $PuCoGa_5$. The Fermi energy falls on the right-hand side of a narrow $5f$ peak. Magnetic

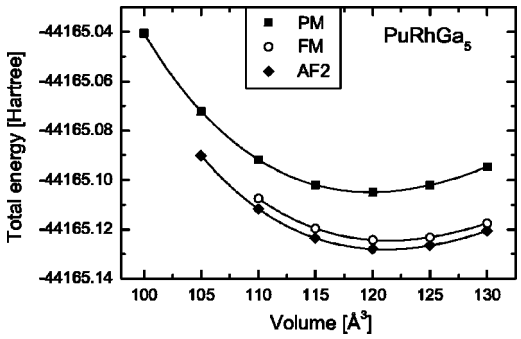

FIG. 6. Total energy *versus* volume calculated for the PM, FM, and AF2 phases of $PuRhGa_5$.

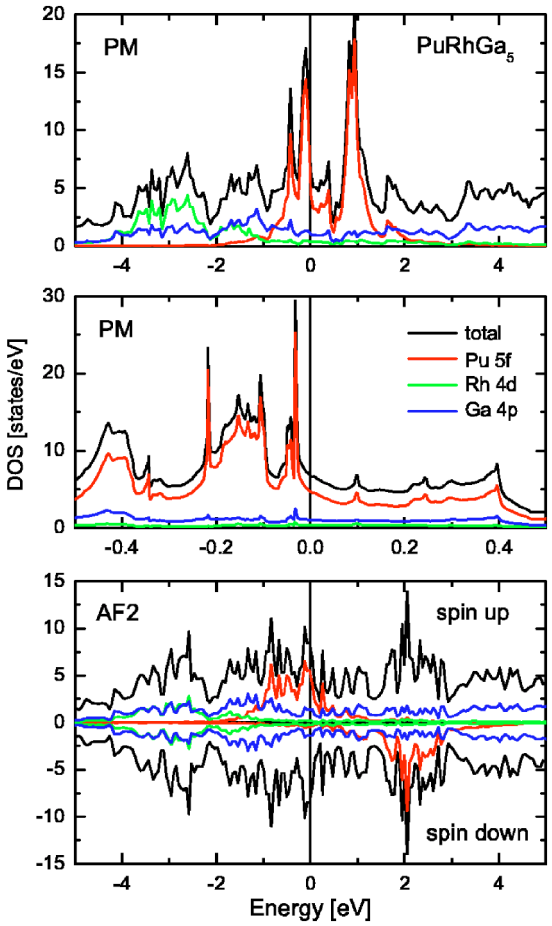

FIG. 7. (Color online) Calculated total and partial DOS of $PuRhGa_5$ in the PM phase (top and middle panel) and in the AF2 phase (bottom panel), for the experimental lattice constant. Only the spin-projected partial DOS of one AF atom-type is shown.

ordering causes a significant splitting of the $5f$ partial DOS and concurrent reduction of the DOS peak at E_F. The unenhanced specific-heat coefficient of PM $PuRhGa_5$ $\gamma = 16.5$ mJ/mol K^2 is calculated to be smaller than that of $PuCoGa_5$ (which is about 30 mJ/mol K^2, Ref. 25). First measurements, however, indicate for $PuRhGa_5$ a γ-value that is similar to that of $PuCoGa_5$ (Ref. 53). If this is confirmed, the smaller T_c of $PuRhGa_5$ could only be due to a pairing potential that is weaker for $PuRhGa_5$. As is discussed below, the pairing potential might depend sensitively on the c/a ratio.

The energy bands are shown in Fig. 4. Note, that compared to $PuCoGa_5$ there exist some small modifications in the energy bands near E_F. Along the $\Gamma - X$ high-symmetry line there is one band (No. 89 in our calculations) which lies barely above E_F. Hence, the topology of the Fermi surface changes along this symmetry axis: instead of the two disjunct Fermi surface sheets shown in Fig. 5, these sheets merge and form one larger sheet (not shown). Consequently, also the extremal orbits in the $z=0$ plane are different: instead of the two extremal orbits denoted β and γ, there is now one large orbit (denoted γ') centered at the M point. The dHvA quantities calculated for $PuRhGa_5$ are given in Table II. Except for the mentioned orbits, the computed dHvA frequencies and masses are comparable to those of $PuCoGa_5$.

TABLE II. Theoretical de Haas-van Alphen frequencies F and effective masses m of paramagnetic $PuRhGa_5$, calculated for the experimental lattice parameters and for H parallel to the c axis. The symbols labeling the extremal orbits are shown in Fig. 5.

Symbol	Center (band)	F (kT)	m (m_e)
α	$\Gamma(87)$	1.608	−1.092
γ'	$M(89)$	13.809	5.295
δ	$Z(89)$	6.098	−2.910
ξ	$M(91)$	5.059	3.826
ζ	$A(91)$	5.309	2.992
σ	$M(93)$	1.541	1.362
τ	$A(93)$	1.945	0.987

C. $PuIrGa_5$

Very recently, the first experimental data on $PuIrGa_5$ were reported.[4] Although more research is definitely required, the first investigations indicate that $PuIrGa_5$ displays a physical behavior *distinct* from both $PuCoGa_5$ and $PuRhGa_5$. $PuIrGa_5$ does not become a superconductor down to 2 K, instead antiferromagnetic ordering seems to occur below 17 K.[4] This finding indicates a cross-over from weak antiferromagnetic fluctuations in $PuCoGa_5$ and $PuRhGa_5$ to a stronger antiferromagnetic interaction in $PuIrGa_5$, something which could shed light on the origin of the unexpected superconductivity.

In Fig. 8 we present the calculated total energies for $PuIrGa_5$. Again the LSDA approach predicts the AF2 phase to be favored. The calculated equilibrium lattice parameters are $a=4.27$ Å, $c/a=1.567$, and $z(\mathrm{Ga})=0.293$, which are to be compared to the experimental values[4] $a=4.324$ Å, $c/a=1.576$, and $z(\mathrm{Ga})=0.302$, respectively. The equilibrium lattice parameters are thus also in the case of $PuIrGa_5$ quite well explained by the LSDA approach (the calculated a is 1.25% smaller). The predicted AF order is in accordance with experiment, too. Further experimental investigations are needed to determine what type of AF order exactly occurs in $PuIrGa_5$. $PuIrGa_5$ also deviates from the Co and Rh compounds for what concerns the susceptibility and resistivity.

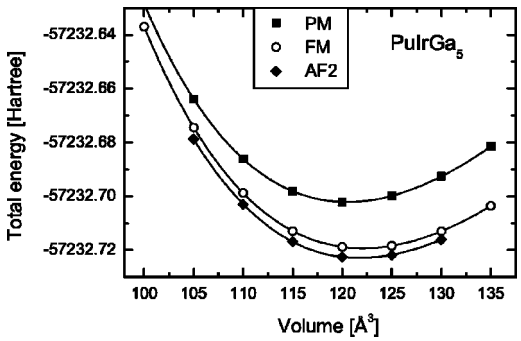

FIG. 8. The same as Fig. 6, but for $PuIrGa_5$.

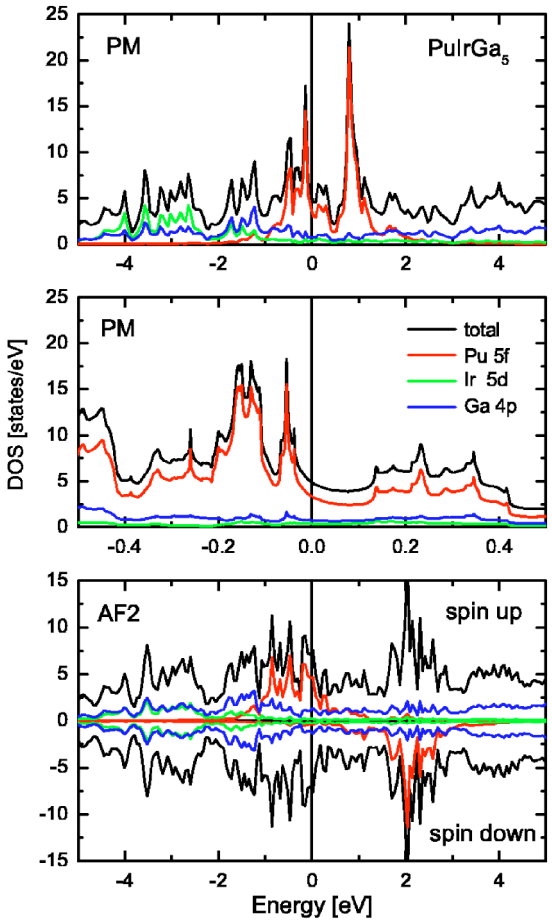

FIG. 9. (Color online) The same as Fig. 7, but for $PuIrGa_5$.

At elevated temperatures the susceptibility displays Curie-Weiss behavior, but the effective moment is estimated[4] to be 0.33 μ_B, which is thus considerably reduced from the Pu^{3+} value. The S-shaped upturn in the resistivity is found to be smaller for $PuIrGa_5$ than for the other two Pu-115 compounds.

The partial DOS of $PuIrGa_5$—calculated for the experimental lattice parameters—is shown in Fig. 9. As could be expected, the DOS is similar to that of the Co and Rh compounds. The DOS at E_F in the PM phase is lower than that of $PuRhGa_5$ and $PuCoGa_5$. The calculated, unenhanced specific-heat coefficient is only $\gamma = 11.6$ mJ/mol K^2. This is a consequence of the sharp $5f$ peak in the nonmagnetic phase moving successively to a position deeper below E_F from the Co to the Ir compound. The main resonance of the Ir $5d$ states occurs at a binding energy larger than 2 eV, which is more than the binding energy of the Co $3d$ states in $PuCoGa_5$. The energy bands of $PuIrGa_5$ in the AF2 phase have been calculated, but we refrain from showing the band structure here for brevity's sake and also because the experimental antiferromagnetic structure is not yet known.

For comparison to the other Pu-115 compounds we provide in Table III the calculated dHvA quantities of paramagnetic $PuIrGa_5$. The Fermi surface of $PuIrGa_5$ is nearly identical to that of $PuCoGa_5$. The Fermi surface sheet due to band 93 (the thinner tube in Fig. 5) is somewhat thicker in between the M and A points, thus an additional extremal orbit—denoted by τ'—occurs on this sheet. The dHvA quantities of $PuIrGa_5$ in the PM phase could be highly relevant for investigating the cross-over from the nonsuperconducting, antiferromagnetic phase to the nonmagnetically ordered, superconducting phase. For the related superconductor $CeRhIn_5$ it was discovered that a modest pressure of 16 kbar was sufficient to surpress the antiferromagnetic order and induce superconductivity.[17] Exploiting dHvA measurements under pressure, the changes of the Fermi surface in going from one phase to another were thereby investigated.[54]

TABLE III. The same as Table II, but for paramagnetic $PuIrGa_5$.

Symbol	Center (band)	F (kT)	m (m_e)
α	$\Gamma(87)$	0.854	−0.751
β	$X(89)$	0.087	−0.836
γ	$M(89)$	3.379	−1.742
δ	$Z(89)$	7.529	−2.168
ξ	$M(91)$	4.870	3.099
ζ	$A(91)$	4.197	2.710
σ	$M(93)$	1.447	0.907
τ	$A(93)$	1.267	1.087
τ'	$k_z = 0.12(93)$	1.563	1.075

D. $UCoGa_5$

$UCoGa_5$ samples were first prepared and investigated one decade ago.[7,9] More recently, results on purer single crystals were reported.[11] The earlier as well as most recent examinations show that $UCoGa_5$ is a weakly temperature dependent paramagnet, displaying no Curie-Weiss behavior.[55,56] In the latter respect exhibits $UCoGa_5$ a $5f$ behavior quite comparable to that of UGa_3, which constitutes the essential building block of the $UCoGa_5$ unit cell. UGa_3 is known to be an itinerant $5f$ antiferromagnet (see, e.g., Refs. 57–60), without Curie-Weiss behavior detected up to 900 K. A remarkable feature of $UCoGa_5$ is its low specific-heat coefficient of about 5 mJ/mol K^2 (Refs. 5, 9, and 11). In itself, a small γ-value has sometimes been regarded as a sign of localized $5f$ states, but we shall see below that this is not necessarily the case. The dHvA quantum oscillations in $UCoGa_5$ were recently studied, from which small Fermi surface portions were inferred.[11,61]

For $UCoGa_5$ our self-consistent calculations always converged to the paramagnetic solution, in agreement with the experimentally observed PM ground state. The optimized theoretical lattice parameters are $a = 4.146$ Å, $c/a = 1.59$, and $z(\mathrm{Ga}) = 0.306$. These values compare reasonably well (2% deviation) with the experimental[7,9] data $a = 4.234$ Å, $c/a = 1.588$, and $z(\mathrm{Ga}) = 0.3048$, respectively. In Fig. 10 we show the calculated DOS of paramagnetic $UCoGa_5$. The Fermi level falls precisely in a quasi-gap of the DOS. This quasi-gap is due to $5f$ hybridization and not due to the spin-orbit splitting of the $f_{5/2}$ and $f_{7/2}$ subbands, which occurs 0.7 eV

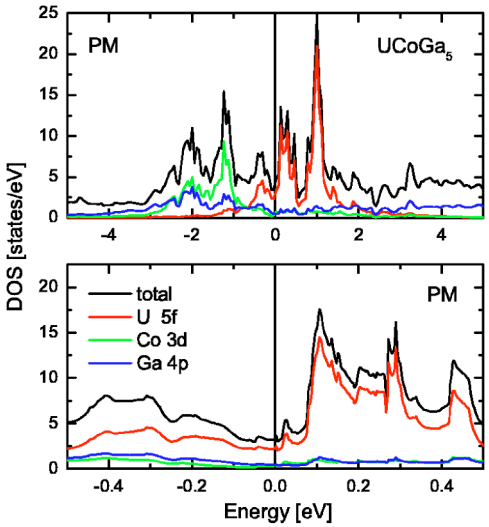

FIG. 10. (Color online) Calculated total and partial DOS of paramagnetic $UCoGa_5$, adopting the experimental lattice parameters. Note that the Fermi level falls in a quasi-gap of the DOS.

above E_F. As a consequence, the calculated band-structure specific-heat coefficient is small, $\gamma = 7.0$ mJ/mol K^2, in agreement with experiment. The measured γ-values range from about 3.5 mJ/mol K^2 (Refs. 5 and 11) to 10 mJ/mol K^2 (Ref. 9). Similar to the situation we already noted for $PuCoGa_5$, the Co 3*d* states of $UCoGa_5$ are practically filled. The states in the vicinity of the Fermi energy are therefore dominated by the uranium 5*f* states, with an admixture of Ga 4*p* states. The corresponding energy-band structure is shown in Fig. 11. The uranium 5*f* character of the bands is highlighted by the fatness of the respective bands, proving that in spite of the quasi-gap the bands about E_F consist mainly of 5*f* states. Our band structure is in good agreement with that reported recently by Maehira *et al.*,[26] except for the location of some bands about the *M* point. Our result is significantly different from another recent investigation.[55] In our relativistic calculation the U 5*f* DOS is spin-orbit split (see Fig. 10), but such a splitting does not seem to be present in the 5*f* DOS of Ref. 55.

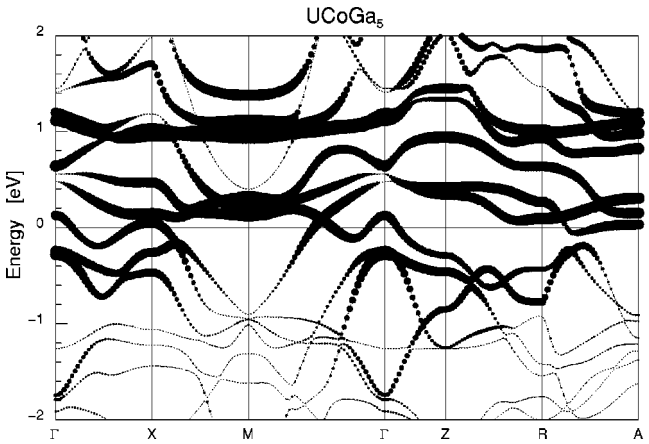

FIG. 11. Calculated energy bands of paramagnetic $UCoGa_5$ in the vicinity of the Fermi level. The amount of 5*f* character in each of the bands is indicated by the fatness of the band.

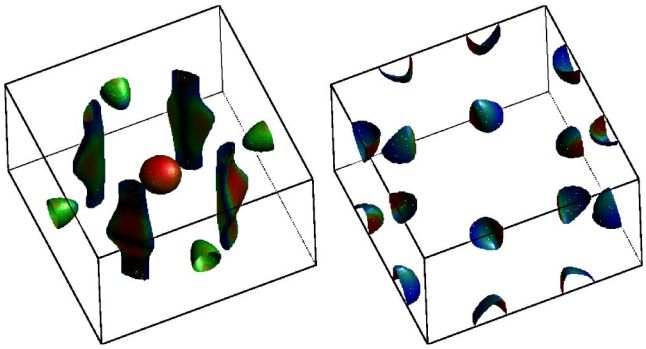

FIG. 12. (Color online) The calculated Fermi surface of $UCoGa_5$. The Fermi surface sheets in the left-hand panel correspond to band No. 87, those in the right-hand panel to band No. 89.

Recent dHvA measurements detected three extremal orbits for $UCoGa_5$, which were attributed to small, closed Fermi surface sheets.[11] The *ab initio* calculated Fermi surface, shown in Fig. 12, does consist of three small, closed Fermi surface portions (centered at the Γ, *X*, and *T* point, respectively), but in addition there is a tube-like sheet (connecting the so-called Σ and *S* points[62] in the BZ). Another recent *ab initio* calculation,[61] also performed for the experimental lattice parameters, provided a very similar Fermi surface. The four tube-like sheets, however, are smaller and have shrunk to four disconnected Fermi surface portions centered in the $z=0$ plane near the Σ point. In Table IV the experimental dHvA quantities as well as the results of our calculation are given. The calculated dHvA quantities are quite small, however, the dHvA quantities corresponding to the Fermi surfaces at the *X* point and the *T* point are 2–3 times larger than the experimental values. These small Fermi surfaces are probably sensitive to the lattice constants and likely also to aspects of the band-structure method (cf. Ref. 61).

Altogether, the physical properties of $UCoGa_5$ are well explained by the delocalized 5*f* description. This strongly suggestes that $UCoGa_5$ is—like UGa_3—an itinerant 5*f* material.

E. $NpCoGa_5$

Only very recently $NpCoGa_5$ has been synthesized.[5] The first investigations reveal that $NpCoGa_5$ orders antiferromag-

TABLE IV. Experimental and calculated de Haas-van Alphen frequencies *F* (in kT) and effective masses *m*(in m_e) of $UCoGa_5$ for *H* parallel to the *c* axis.

	Experiment[a]		Calculation	
Center (band)	*F*	$\|m\|$	*F*	*m*
Γ(87)	0.741	0.82	0.566	−0.641
X(87)	0.203	1.3	0.497	−0.831
T(89)	0.166	1.35	0.493	1.539
Σ(87)	—	—	0.359	−0.569
S(87)	—	—	0.140	−0.504

[a]Reference 11.

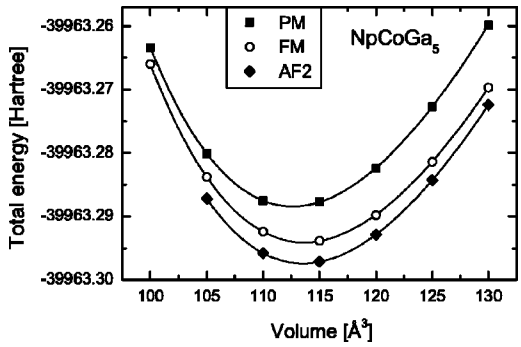

FIG. 13. The same as Fig. 6, but for $NpCoGa_5$.

netically below $T_N=47$ K and superconductivity is not observed down to 0.4 K. At elevated temperatures the susceptibility obeys a modified Curie-Weiss law with a reduced effective moment (as compared to the free-ion value) of $\mu_{eff}\approx 1.4\ \mu_B$.[5]

The calculated total energies for the different magnetic phases are presented in Fig. 13. We observe readily that the AF phase is predicted to be the ground state, in accordance with the experimentally observed AF order. Also the computed equilibrium lattice parameters $a=4.1322$ Å, $c/a=1.61$, and $z(\mathrm{Ga})=0.305$ correspond fairly well (2.5% deviation) to the experimental values,[5] which are $a=4.2377$ Å, $c/a=1.602$, and $z(\mathrm{Ga})=0.3103$, respectively. This deviation—being the largest that we found for the studied actinide-115 materials—could be improved by employing the GGA approach. The DOS, calculated for the experimental lattice parameters, is shown in Fig. 14. In the PM phase the DOS exhibits a sharp peak precisely at E_F. Such a high DOS peak usually indicates an instability that can be removed by a symmetry breaking, for example, magnetic ordering. Indeed, the DOS at E_F is much reduced for the FM and AF2 phases. The exchange splitting of the Np $5f$ states pushes a part of the $5f$ spin up DOS to higher binding energies, while the spin down DOS is shifted above E_F. In all three magnetic phases the contribution of the Np $5f$'s dominates the DOS in the vicinity of E_F. The unenhanced linear specific-heat coefficient, calculated for the AF2 phase, is $\gamma=30.7$ mJ/mol K^2. This value is half the measured value, $\gamma\approx 60$ mJ/mol K^2 (Ref. 5).

The calculated magnetic moments of $NpCoGa_5$ in the AF2 phase are given in Table V. The calculated orbital moment on Np compensates to a large extent the spin moment. This we find to be the case even more for $NpCoGa_5$ in the FM phase, where the spin moment (2.86 μ_B) and orbital moment (−2.81 μ_B) nearly cancel each other. The *ab initio* calculated magnetic moment on neptunium is 0.85 μ_B for the AF2 phase, which compares surprisingly well to the first experimental value for the Np moment,[5] 0.84 μ_B. This agreement could, however, be fortuitous, as the LSDA often underestimates the orbital moment. In early actinides the size of the orbital moment is usually larger than the spin moment, as follows from the shape of the neutron form factor. Corrections to the LSDA as, e.g., the orbital polarization[27] are then needed to improve the size of the orbital moment.

The *ab initio* calculated band structures of $NpCoGa_5$ in both the PM and AF2 phases are shown in Fig. 15. In both phases there are Np $5f$ related bands that are practically dispersionless close to the Fermi energy along some high-symmetry lines. The amount of $5f$ character is displayed by the fatness of the bands. The energy bands of PM $NpCoGa_5$ were recently calculated by Maehira *et al.*[26] Their band structure is quite similar to ours, with the exception of the bands near the M point. A small difference exists also along the $R-A$ high-symmetry direction, where in Ref. 26 a band lies below E_F, which is just above E_F in our calculation.

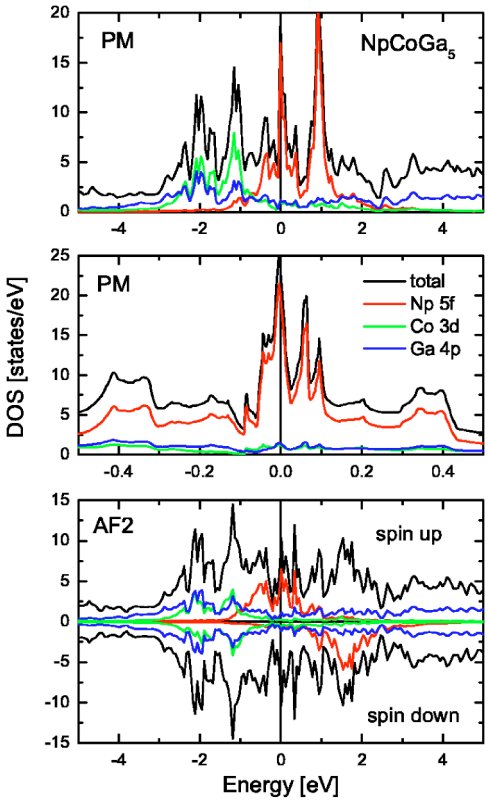

FIG. 14. (Color online) The same as Fig. 7, but for $NpCoGa_5$.

Although it can be anticipated that the Np $5f$ electrons have a stronger tendency towards localization than those of U in $UCoGa_5$, the good correspondence between theory and experiment for the main physical properties of $NpCoGa_5$ substantiates that the Np $5f$ behavior is nevertheless correctly captured by the LSDA description.

F. $AmCoGa_5$

Very recently, the first samples of $AmCoGa_5$ in the $HoCoGa_5$ structure have been prepared.[6] $AmCoGa_5$ is a

TABLE V. Calculated magnetic spin (M_s) and orbital moments (M) (in μ_B) of $NpCoGa_5$ in the AF2 phase, adopting the experimental lattice constants.

	Np	Co	Ga	total
M_s (μ_B)	±3.27	±0.33	0.00	±3.60
M_l (μ_B)	∓2.42	0.00	0.00	∓2.42

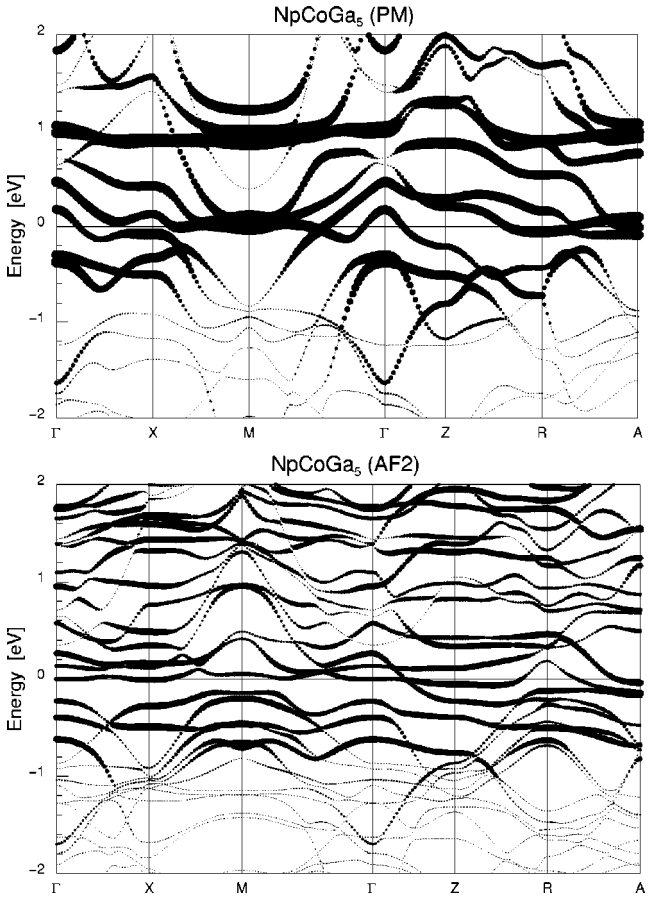

FIG. 15. The calculated LSDA energy bands of $NpCoGa_5$ in the nonmagnetic phase (top panel) and in the AF2 phase (bottom panel). The fatness of the bands indicates the amount of Np $5f$ character in each energy band. In the AF2 phase the $5f$ amount due to only one Np atom is depicted.

temperature-independent paramagnet which does not become superconducting down to 2 K. The former indicates that the Am $5f_{5/2}$ subshell is completely filled, i.e., the $5f$ states are in a $J=0$, $5f^6$ configuration, consistent with the absence of magnetism. We expect the Am $5f$ states to be localized in $AmCoGa_5$. In general not much is known about the behavior of the Am $5f$ electrons. So far only Am metal and a few Am compounds have been investigated.[28,63,64] Photoelectron spectroscopy provided evidence for localized $5f$ electrons in Am metal.[28] Only under pressures above 10 GPa have signs of delocalization of the $5f$ electrons been observed.[64] It is thus reasonable to assume localized $5f$ electrons for $AmCoGa_5$. Consequently, we have calculated the electronic structure of $AmCoGa_5$ employing the $5f$ core approach. In this approach, the equilibrium lattice parameters cannot reliably be calculated since important contributions to the total energy are ignored. As also no experimental lattice constants are known we computed the band structure for several sets of estimated lattice constants (results are not shown here for the sake of conciseness). Our calculations show that some parts of the computed band structure are similar to those of the other actinide-115 compounds. In the vicinity of the Fermi energy, however, three bands are missing, which affects the band structure considerably near the A and M points. At the M point some very dispersive bands are in addition pulled below E_F. The Fermi surface topology is thus significantly different from that of $PuCoGa_5$. Further investigations of $AmCoGa_5$ have to await more experimental information becoming available.

IV. DISCUSSION AND CONCLUSIONS

From the foregoing results a clear trend in the behavior of the actinide $5f$ electrons in the 115 compounds emerges. The physical properties of $UCoGa_5$ and $NpCoGa_5$ are relatively well described by the delocalized LSDA approach. The lattice parameters of the three Pu-115 compounds are properly explained by the LSDA approach as well. For $AmCoGa_5$ the situation is different: although experimental information is lacking, we expect the Am $5f$'s to be localized. The recent photoemission study[40] of $PuCoGa_5$ confirmed the presence of Pu $5f$ electrons at E_F. However, the photoemission spectrum shows a second f-related response at a binding energy of 1.1 eV. The latter response has been interpreted as originating from semi-localized $5f$ electrons.[40] Thus, it could be that in reality some of the $5f$ electrons are quasi-localized while others are delocalized. Such a scenario has been discussed earlier[30,35] for δ-Pu and it could be valid for $PuCoGa_5$ as well.[65] However, we note that in the magnetic phases there is a substantial exchange splitting of the $5f$ states leading to a $5f$ contribution at higher binding energies (see Fig. 3). Other techniques and more experiments are therefore needed to establish to what extent the $5f$'s are localized.

Our band-structure calculations predict several properties for the Pu-115 compounds that have implications for explaining the unexpected superconductivity. One of these is the presence of Pu $5f$ states at the Fermi energy. As a consequence, the Pu $5f$ electrons participate in the Cooper pair formation.[25] A second important finding is the predicted AF order, which does occur for $PuIrGa_5$. The observation of AF order and the absence of superconductivity in $PuIrGa_5$ indicates the cross-over that takes place in the Pu-115 series. According to the calculations, antiferromagnetic interactions can be expected to be present in all three Pu-115 compounds. A trade-off with the superconducting order will determine which order will become the one with the lowest energy. The stronger AF interaction in $PuIrGa_5$ makes antiferromagnetism favorable over superconductivity, whereas for the weaker AF interactions in $PuCoGa_5$ and $PuRhGa_5$ superconductivity can prevail over AF order. Possibly the pair formation could benefit from the AF spin fluctuations which then could be the as yet unidentified unconventional pairing mechanism.

The discovery of AF order in $PuIrGa_5$ re-inforces the remarkable analogy to the Ce-115 heavy-fermion superconductors. Antiferromagnetic order also occurs for one compound ($CeRhIn_5$) in the Ce-115 series, while $CeCoIn_5$ and $CeIrIn_5$ do not order magnetically but become superconductors at low temperatures.[17–19] Under pressure AF ordering can be destroyed in $CeRhIn_5$, upon which superconductivity sets in. It would be of interest to examine if a similar behavior takes place also in $PuIrGa_5$ under pressure. Another analogy

of the Ce-115 and Pu-115 materials is the very high upper critical field H_{c2}. For $CeCoIn_5$ the upper critical field exceeds the Clogston limit,[66] however Pauli limiting of H_{c2} does set in at low temperatures. Accordingly, the superconducting order parameter was determined to exhibit unconventional spin singlet, *d*-wave symmetry. The upper critical field of $PuCoGa_5$ was reported[1] to exceed the Clogston limit as well, but, because the required field was too high ($\approx$74 T) to be reached experimentally, H_{c2} could not be measured down to zero temperature. It could thus be that for $PuCoGa_5$ Pauli limiting also sets in at low temperatures, which would definitely provide support for spin singlet, possibly *d*-wave pairing. This hypothesis could be tested on $PuRhGa_5$, for which the lower T_c of 8.5 K might allow H_{c2} to be measured down to zero temperature. Once this can be carried out, it would also be of interest to measure the crystallographic anisotropy of H_{c2}, which could give clues about the proposed quasi-two-dimensionality of the Fermi surface and possibly concerning nodes in the gap.[25] Of course, evidence for unconventional superconductivity and even the symmetry of the gap could be obtained from various other measurements (nuclear magnetic and quadrupole resonance, thermal conductivity, penetration depth, and specific heat). Such measurements, which have not been performed as yet, would ideally require a nonradioactive ^{242}Pu-115 sample. We note, however, that even in the case that an unconventional symmetry of the gap would be discovered, this is not sufficient to conclude that an unconventional pairing mechanism is responsible.[67]

A further analogy to the Ce-115 materials is the dependence of T_c on the c/a ratio. An amazingly sensitive, linear dependence of T_c on the c/a ratio was found for the Ce-115 compounds:[68] changes in the c/a ratio of only 2% cause T_c to change by a factor of five. As is the case for the Ce-115 series, within the Pu-115 series the c/a ratio also decreases with an increasing transition-metal ion radius, from 1.603 for $PuCoGa_5$ to 1.594 for $PuRhGa_5$ and to 1.576 for $PuIrGa_5$. This trend is well reproduced by our *ab initio* calculations, which give 1.602, 1.590, and 1.567, respectively. A linear interpolation of the T_c as a function of c/a for $PuCoGa_5$ and $PuRhGa_5$ immediately reveals that for the c/a of $PuIrGa_5$ the corresponding T_c will be zero. Moreover, both the Ce-115 and Pu-115 compounds have the same huge slope $d \ln T_c/d(c/a) \approx 80$ K, suggesting similar underlying physics.[69] The sensitive dependence of T_c on the c/a ratio in the Ce-115 compounds has not yet been explained microscopically. In the quasi-two-dimensional structure the Ce-planes are most likely magnetically nearly decoupled. In such a situation the AF spin fluctuations would depend delicately on the interlayer distance. The Pu interlayer coupling of $PuCoGa_5$ has been calculated to be very weak as well (cf. Fig. 2). One could thus speculate that AF spin fluctuations play a role in the Cooper pair formation (see, e.g., Refs. 19 and 70). As we noted before, in the Pu-115 compounds $5f$ electrons occur at the Fermi energy and are stronger hybridized than the Ca $4f$'s. Although the quasi-particle density of states at E_F is larger for the Ce-115 compounds, the much stronger hybridization of the Pu $5f$'s could nevertheless explain a stronger coupling constant, which would lead to a higher T_c.

ACKNOWLEDGMENTS

It is a pleasure to thank Joe Thompson, John Sarrao, Tomasz Durakiewicz (Los Alamos, NL) and Gerry Lander, Franck Wastin, Pascal Boulet, Eric Colineau, Jean Rebizant, Jean-Christophe Griveau, and Pavel Javorský (ITU, Karlsruhe) for valuable discussions and for disclosing information to us prior to publication. We also gratefully acknowledge discussions with Alexander Shick, Olle Eriksson, Roland Hayn, Stefan-Ludwig Drechsler, and Manuel Richter. This work was supported financially by the Egyptian Ministry of Higher Education and Scientific Research and the EC, RTN-Network Psi-k f-electron.

[1] J. L. Sarrao, L. A. Morales, J. D. Thompson, B. L. Scott, G. R. Stewart, F. Wastin, J. Rebizant, P. Boulet, E. Colineau, and G. H. Lander, Nature (London) **420**, 297 (2002).

[2] F. Wastin, P. Boulet, J. Rebizant, E. Colineau, and G. H. Lander, J. Phys.: Condens. Matter **15**, S2279 (2003).

[3] J. C. Griveau, C. Pfleiderer, P. Boulet, J. Rebizant, and F. Wastin J. Magn. Magn. Mater. **272–276**, 154 (2004).

[4] F. Wastin, D. Bouëxière, P. Boulet, E. Colineau, J. C. Griveau, and J. Rebizant (unpublished).

[5] E. Colineau, P. Boulet, F. Wastin, and J. Rebizant (unpublished); E. Colineau, P. Javorský, P. Boulet, F. Wastin, J. C. Griveau, J. Rebizant, J. P. Sanchez, and G. R. Stewart, Phys. Rev. B **69**, 184411 (2004).

[6] F. Wastin (private communication, 2003).

[7] Yu. N. Grin, P. Rogl, and K. Hiebl, J. Less-Common Met. **121**, 497 (1986).

[8] V. Sechovský, L. Havela, G. Schaudy, G. Hilscher, N. Pillmayer, and P. Rogl, J. Magn. Magn. Mater. **104–107**, 11 (1992).

[9] J. S. Noguchi and K. Okuda, J. Magn. Magn. Mater. **104–107**, 57 (1992).

[10] Y. Tokiwa, Y. Haga, E. Yamamoto, D. Aoki, N. Watanabe, R. Settai, T. Inoue, K. Kindo, H. Harima, and Y. Ōnuki, J. Phys. Soc. Jpn. **70**, 1744 (2001).

[11] S. Ikeda, Y. Tokiwa, T. Okubo, Y. Haga, E. Yamamoto, Y. Inada, R. Settai, and Y. Ōnuki, J. Nucl. Sci. Technol. **3**, 206 (2002).

[12] M. Nakashima, Y. Tokiwa, H. Nakawaki, Y. Haga, Y. Uwatoko, R. Settai, and Y. Ōnuki, J. Nucl. Sci. Technol. **3**, 214 (2002).

[13] Y. Tokiwa, Y. Haga, N. Metoki, A. Nakamura, Y. Ishii, and Y. Ōnuki, J. Nucl. Sci. Technol. **3**, 210 (2002).

[14] Y. Ōnuki, Y. Haga, E. Yamamoto, Y. Inada, R. Settai, H. Yamagami, and H. Harima, J. Phys.: Condens. Matter **15**, S1903 (2003).

[15] K. Kaneko, N. Metoki, N. Bernhoeft, G. H. Lander, Y. Ishii, S. Ikeda, Y. Tokiwa, Y. Haga, and Y. Ōnuki, Phys. Rev. B **68**, 214419 (2003).

[16] S. Julian, Phys. World 20 (2003).

[17] H. Hegger, C. Petrovic, E. G. Moshopoulou, M. F. Hundley, J. L. Sarrao, Z. Fisk, and J. D. Thompson, Phys. Rev. Lett. **84**, 4986

(2000).
[18] C. Petrovic, R. Movshovich, M. Jaime, P. G. Pagliuso, M. F. Hundley, J. L. Sarrao, Z. Fisk, and J. D. Thompson, Europhys. Lett. **53**, 354 (2001).
[19] C. Petrovic, P. G. Pagliuso, M. F. Hundley, R. Movshovich, J. L. Sarrao, J. D. Thompson, Z. Fisk, and P. Monthoux, J. Phys.: Condens. Matter **13**, L337 (2001).
[20] W. Bao, P. G. Pagliuso, J. L. Sarrao, J. D. Thompson, Z. Fisk, J. W. Lynn, and R. W. Erwin, Phys. Rev. B **62**, R14 621 (2000).
[21] G.-q. Zheng, K. Tanabe, T. Mito, S. Kawasaki, Y. Kitaoka, D. Aoki, Y. Haga, and Y. Ōnuki, Phys. Rev. Lett. **86**, 4664 (2001).
[22] R. Movshovich, M. Jaime, J. D. Thompson, C. Petrovic, Z. Fisk, P. G. Pagliuso, and J. L. Sarrao, Phys. Rev. Lett. **86**, 5152 (2001).
[23] K. Izawa, H. Yamaguchi, Y. Matsuda, H. Shishido, R. Settai, and Y. Ōnuki, Phys. Rev. Lett. **87**, 057002 (2001).
[24] R. J. Ormeno, A. Sibley, C. E. Gough, S. Sebastian, and I. R. Fisher, Phys. Rev. Lett. **88**, 047005 (2002).
[25] I. Opahle and P. M. Oppeneer, Phys. Rev. Lett. **90**, 157001 (2003).
[26] T. Maehira, T. Hotta, K. Ueda, and A. Hasegawa, Phys. Rev. Lett. **90**, 207007 (2003).
[27] M. S. S. Brooks and B. Johansson, *in Handbook of Magnetic Materials*, edited by K. H. J. Buschow (North-Holland, Amsterdam, 1993), Vol. 7, p. 139.
[28] J. R. Naegele, L. Manes, J. C. Spirlet, and W. Müller, Phys. Rev. Lett. **52**, 1834 (1986).
[29] B. Sadigh, P. Söderlind, and W. G. Wolfer, Phys. Rev. B **68**, 241101(R) (2003).
[30] O. Eriksson, J. D. Becker, A. V. Balatsky, and J. M. Wills, J. Alloys Compd. **287**, 1 (1999).
[31] J. Bouchet, B. Siberchicot, F. Jollet, and A. Pasturel, J. Phys.: Condens. Matter **12**, 1723 (2000).
[32] S. Y. Savrasov and G. Kotliar, Phys. Rev. Lett. **84**, 3670 (2000).
[33] P. Söderlind, Europhys. Lett. **55**, 525 (2001); P. Söderlind, A. Landa, and B. Sadigh, Phys. Rev. B **66**, 205109 (2002).
[34] S. Y. Savrasov, G. Kotliar, and E. Abrahams, Nature (London) **410**, 793 (2001).
[35] J. M. Wills, O. Eriksson, A. Delin, P. H. Andersson, J. J. Joyce, T. Durakiewicz, M. T. Butterfield, A. J. Arko, D. P. Moore, and L. A. Morales, J. Electron Spectrosc. Relat. Phenom. **135**, 163 (2004).
[36] T. Gouder, F. Wastin, J. Rebizant, and L. Havela, Phys. Rev. Lett. **84**, 3378 (2000).
[37] P. M. Oppeneer, T. Kraft, and M. S. S. Brooks, Phys. Rev. B **61**, 12 825 (2000).
[38] V. Ichas, J. C. Griveau, J. Rebizant, and J. C. Spirlet, Phys. Rev. B **63**, 045109 (2001).
[39] P. Wachter, M. Filzmoser, and J. Rebizant, Physica B **296**, 199 (2001).
[40] J. J. Joyce, J. M. Wills, T. Durakiewicz, M. T. Butterfield, E. Guziewicz, J. L. Sarrao, L. A. Morales, A. J. Arko, and O. Eriksson, Phys. Rev. Lett. **91**, 176401 (2003).
[41] I. Opahle, Ph.D. thesis, University of Technology Dresden, 2001.
[42] H. Eschrig, M. Richter, and I. Opahle, in *Relativistic Electronic Structure Theory—Part II: Applications*, edited by P. Schwerdtfeger (Elsevier, Amsterdam, 2004), pp. 723–776.
[43] K. Koepernik and H. Eschrig, Phys. Rev. B **59**, 1743 (1999).
[44] J. P. Perdew and Y. Wang, Phys. Rev. B **45**, 13 244 (1992).
[45] Measurements on another sample gave $a=4.235$ Å, $c/a=1.604$, and $z(\mathrm{Ga})=0.3086$ (Ref. 2).
[46] D. J. Lamm and S.-K. Chan, Phys. Rev. B **6**, 307 (1972).
[47] J. C. Lashley, J. Singleton, A. Migliori, J. B. Betts, R. A. Fisher, J. L. Smith, and R. J. McQueeney, Phys. Rev. Lett. **91**, 205901 (2003).
[48] U. Alver, R. G. Goodrich, N. Harrison, D. W. Hall, E. C. Palm, T. P. Murphy, S. W. Tozer, P. G. Pagliuso, N. O. Moreno, J. L. Sarrao, and Z. Fisk, Phys. Rev. B **64**, 180402(R) (2001).
[49] D. Hall, E. Palm, T. Murphy, S. Tozer, E. Miller-Ricci, L. Peabody, C. Quay Huei Li, U. Alver, R. G. Goodrich, J. L. Sarrao, P. G. Pagliuso, J. M. Wills, and Z. Fisk, Phys. Rev. B **64**, 064506 (2001).
[50] H. Shishido, R. Settai, D. Aoki, S. Ikeda, H. Nakawaki, N. Nakamura, T. Iizuka, Y. Inada, K. Sugiyama, T. Takeuchi, K. Kindo, T. C. Kobayasi, Y. Haga, H. Harima, Y. Aoki, T. Namiki, H. Sato, and Y. Ōnuki, J. Phys. Soc. Jpn. **71**, 162 (2002).
[51] Y. Ōnuki, Y. Tokiwa, S. Ikeda, D. Aoki, Y. Inada, R. Settai, T. Maehira, E. Yamamoto, and Y. Haga, J. Nucl. Sci. Technol. **3**, 114 (2002).
[52] The dHvA quantities are calculated numerically by computing the Fermi velocities on mesh of k-points along the orbit and by a subsequent Romberg integration [see P. M. Oppeneer and A. Lodder, J. Phys. F: Met. Phys. **17**, 1901 (1987)] .
[53] P. Javorský, F. Wastin *et al.* (private communication).
[54] H. Shishido, R. Settai, S. Araki, T. Ueda, Y. Inada, T. C. Kobayashi, T. Muramatsu, Y. Haga, and Y. Ōnuki, Phys. Rev. B **66**, 214510 (2002).
[55] R. Troć, Z. Bukowski, C. Sulkowski, H. Misiorek, J. A. Morkowski, A. Szajek, and G. Chelkowska (unpublished).
[56] The earlier susceptibility measurements (Refs. 7 and 9) showed a low-temperature upturn in the susceptibility, which is not present in the measurement on high-quality single crystals (Ref. 11).
[57] D. Kaczorowski, R. Troć, D. Badurski, A. Böhm, L. Shlyk, and F. Steglich, Phys. Rev. B **48**, 16 425 (1993).
[58] A. L. Cornelius, A. J. Arko, J. L. Sarrao, J. D. Thompson, M. F. Hundley, C. H. Booth, N. Harrison, and P. M. Oppeneer, Phys. Rev. B **59**, 14 473 (1999).
[59] A. Hiess, F. Boudarot, S. Coad, P. J. Brown, P. Burlet, G. H. Lander, M. S. S. Brooks, D. Kaczorowski, A. Czopnik, and R. Troć, Europhys. Lett. **55**, 267 (2001).
[60] D. Aoki, N. Suzuki, K. Miyake, Y. Inada, R. Settai, K. Sugiyama, E. Yamamoto, Y. Haga, Y. Ōnuki, T. Inoue, K. Kindo, H. Sugawara, H. Sato, and H. Yamagami, J. Phys. Soc. Jpn. **70**, 538 (2001).
[61] T. Maehira, M. Higuchi, and A. Hasegawa, J. Phys.: Condens. Matter **15**, S2237 (2003).
[62] For a definition of the notation see, e.g., C. R. Bradley and A. P. Cracknell, *The Mathematical Theory of Symmetry in Solids* (Clarendon, Oxford, 1972).
[63] F. Wastin, J. C. Spirlet, and J. Rebizant, J. Alloys Compd. **219**, 232 (1995).
[64] S. Heathman, R. G. Haire, T. Le Bihan, A. Lindbaum, K. Litfin, Y. Méresse, and H. Libotte, Phys. Rev. Lett. **85**, 2961 (2000).
[65] We remark that even the interpretation of the photoemission spectrum in terms of one-electron densities of states can be wrong if multiplet effects occur [P. Wachter, Solid State Commun. **127**, 599 (2003)].

[66] A. M. Clogston, Phys. Rev. Lett. **8**, 250 (1962).
[67] P. M. Oppeneer and G. Varelogiannis, Phys. Rev. B **68**, 214512 (2003).
[68] P. G. Pagliuso, R. Movshovich, A. D. Bianchi, M. Nicklas, N. O. Moreno, J. D. Thompson, M. F. Hundley, J. L. Sarrao, and Z. Fisk, Physica B **312–313**, 129 (2002).
[69] J. D. Thompson, J. L. Sarrao, L. A. Morales, F. Wastin, and P. Boulet, Physica C (in press), http://dx.doi.org/10.1016/j.physc.2003.11.061
[70] Y. Bang, I. Martin, and A. V. Balatsky, Phys. Rev. B **66**, 224501 (2002).